Odd–even dependence of rectifying behavior in carbon chains modified diphenyl–dimethyl molecule

Qiu-Hua Wu [a], Peng Zhao [a,*], Hai-Ying Liu [a], De-Sheng Liu [b,c], Gang Chen [a,*]

[a] School of Physics and Technology, University of Jinan, Jinan 250022, China
[b] School of Physics, State Key Laboratory of Crystal Materials, Shandong University, Jinan 250100, China
[c] Department of Physics, Jining University, Qufu 273155, China

ABSTRACT

Using density functional theory and non-equilibrium Green's function formalism, we investigate the effects of asymmetric nonequi-length carbon chains on the electron transport properties of diphenyl–dimethyl molecule. The results show significant odd–even dependence: the rectification appears only in the hybrid nanostructure with odd carbon chain on one side and even carbon chain on the other side, while it is negligible in those with odd/even carbon chain on both sides. The mechanism for the odd–even dependence of rectification is analyzed by the bias-dependent transmission spectra, evolution of molecular orbital levels, their spatial distributions, and projected density of states with the applied bias.

© 2014 Elsevier B.V. All rights reserved.

1. Introduction

Low-dimensional carbon-based nanostructures are innovative materials used for molecular devices with the hope for the miniaturization of conventional silicon-based electronic devices to molecular and even atomic scales [1]. For instance, two-dimensional (2D) graphene [2–4], quasi-1D graphene nanoribbons (GNRs) [5–7] and carbon nanotubes (CNTs) [8–10], 0D fullerenes [11–15] and graphene nanoflakes (GNFs) [16–19], have been widely investigated owing to their unique physical and chemical properties and have been utilized in many different devices. Besides, linear carbon chains (CCs) [20–22], which are made up of sp-hybridized carbon atoms and are truely 1D carbon nanostructures, are attracting considerable attention due to their great potential for applications in molecular devices. Theoretically, the most prominent properties, *i.e.*, the odd–even oscillatory conductance behavior, of CCs have been revealed by Lang and Avouris [23,24]. Recently, CCs have been successfully synthesized from GNRs [25] and CNTs [26].

On the other hand, hybrid carbon nanostructures have attracted intense research interests since those hybrid nanostructures may entail certain advantages of their individual components and even create unexpected effects. The first hybrid carbon nanostructure fabricated is the carbon nanopeapods [27–29], in which fullerenes

are enclosed into CNTs. Recently, another kind of hybrid carbon nanostructure, the carbon nanobuds consisting of one or more fullerenes covalently bonded to the sidewall of CNTs, have been successfully prepared [30–32]. On the theoretical side, a new kind of carbon hybrid nanostructure, the carbon dumbbells, in which a CC is connected to two fullerene C_{60}s, have attracted interests from the researchers [33,34]. Wang et al. have performed first-principles transport calculations of those carbon dumbbells and found an obvious metal-insulator-like oscillation with the increase of CCs' length [35]. Very recently, Zhang et al. investigated the electron transport properties of CC-modified donor–acceptor molecules, and found a dramatic odd–even oscillating behavior for the current rectification and negative differential resistance (NDR) with increasing CCs' length [36]. The same authors also studied the electronic structures and transport of CC-modified GNFs, and demonstrated that the rectifying direction would reverse when the number of carbon atoms in the chain changes from odd to even [37]. Mahmoud and Lugli analyzed the transport properties of CC-modified diphenyl–dimethyl molecule, and showed that the NDR behavior can only be observed in the hybrid nanostructures with odd CC [38]. However, in these studies, only symmetric equi-length CCs are used. In the present work, we investigate the effects of asymmetric nonequi-length CCs on the electron transport properties of diphenyl–dimethyl molecule. Our results show that obvious current rectification can only be obtained in the hybrid nanostructures with odd CC on one side and even CC on the other side, while the rectification in those with odd/even CC on both sides is negligible, no matter how the asymmetries are.

* Corresponding authors.
   E-mail addresses: ss_zhaop@ujn.edu.cn (P. Zhao), ss_cheng@ujn.edu.cn (G. Chen).

2. Calculation methods and model

The devices we construct are shown in the inset of Figure 1b. A two-probe system composing of diphenyl–dimethyl molecule with nonequi-length CCs on two sides, capped by two S atoms, is sandwiched between two flat (3×3) Au $(1\,1\,1)$ electrodes. The S atom is located at the hollow site of the Au $(1\,1\,1)$ surface with a typical Au–S distance of 2.45 Å. We consider six models C3C4, C3C5, C3C6, C3C7, C2C4 and C2C6 according to the number of carbon atoms in the chain on the left and right sides, respectively. Clearly, these six models can be divided into three categories in terms of odd–even property of the chain on two sides, i.e., odd–even (C3C4 and C3C6), odd–odd (C3C5 and C3C7), and even–even (C2C4 and C2C6). Geometries of the systems are optimized using quasi-Newton method until all residual forces on each atom are smaller than 0.05 eV/Å.

The geometrical optimizations and the subsequent electron transport calculations are carried out by using the density functional theory (DFT) combined with the non-equilibrium Green's function (NEGF) method as implemented in the ATK package [39,40]. The exchange-correlation potential is described by the Perdew–Burke–Ernzerhof (PBE) formulation of the generalized gradient approximation (GGA) [41]. The Troullier–Martins nonlocal pseudopotentials [42] are employed to represent the atomic core, while single ζ plus polarization (SZP) basis set for Au atoms and double ζ plus polarization (DZP) basis set for other atoms are adopted to expand valence states of electrons. The Hamiltonian, overlaps, and electron densities are evaluated in a real space grid defined with a plane wave cutoff of 150 Ry to achieve a balance between calculation efficiency and accuracy. The current I through a molecular junction as a function of the applied external bias V can be calculated from the Landauer-like formula [43]

$$I(V) = \frac{2e}{h} \int [f(E - \mu_L) - f(E - \mu_R)]T(E, V)\, dE, \qquad (1)$$

where e is the electron charge, h is the Planck's constant, $T(E, V)$ is the transmission probability through the junction for an electron at energy E and an applied bias equals V, $f(E - \mu_{L/R})$ is the Fermi–Dirac distribution function, and $\mu_{L/R}(V) = E_F \pm eV/2$ is the electrochemical potential of the left/right electrode. Since the Fermi level E_F of the system is set to zero, thus the current simply equals to the integral area under the transmission curve within the bias window $[-eV/2, eV/2]$. Furthermore, it is worth mentioning that the case that the left (right) electrode is the anode (cathode) is referred to as

the application of a positive or forward bias. Otherwise, we call it as a negative or reversed bias.

3. Results and discussion

The current–voltage (I–V) characteristics of six models are presented in Figure 1a. We can see that the I–V curves of odd–even models (C3C4 and C3C6) display highly asymmetric behaviors, namely, the currents under positive bias are obvious larger than that under the same negative bias, while these of odd–odd models (C3C5 and C3C7) and even-even models (C2C4 and C2C6) are quasi-symmetric. Besides, the currents of even-even models are obvious weaker than those of odd–even and odd–odd models. The corresponding rectification ratio $R = |I_P/I_N|$, changing with the applied bias for all models, is presented in Figure 1b, where $I_{P/N}$ corresponds to the current under positive/negative bias. Clearly, odd–even models show obvious rectifying behaviors with rectification ratios reaching the maximum values about 7.5 around 1.0 V, while the rectification in those of odd–odd even–even models is negligible. This indicates that one cannot obtain better rectifying performance just by increasing the geometrical asymmetry (i.e., the length difference between CCs on two sides).

As the current is obtained by integrating the transmission spectrum within the bias window, to elucidate the observed odd–even dependence of rectifying behavior, taking models of C3C4, C3C5 and C2C4 as examples, in Figure 2, we plot their bias-dependent transmission spectra in the bias range from −1.0 to 1.0 V in steps of 0.1 V. The zero-bias transmission spectra are marked in red. It is evident that the transmission spectra of three models show distinct features: (1) At equilibrium state, the transmission of C3C4 is very weak in the whole energy region, while C3C5 and C2C4 have an obvious transmission band around and far below the E_F, respectively. (2) When the bias is applied, for C3C4, obvious transmission band appears around the border of μ_L under positive bias window, while the transmission under negative bias window is still very weak. Such a notable asymmetric change of transmission spectrum with respect to different polarities of biases therefore leads to an obvious forward rectification. In contrast, for C3C5 and C2C4, the original transmission band around and far below the E_F decreases with the increase in positive/negative bias, respectively. As a result, the transmission integral under positive bias window is almost the same as that under negative bias window in C3C5 and C2C4. Thus a poor rectification can be expected.

To understand the underlying origins for these transmission peaks and their different changes with applied bias, as shown in
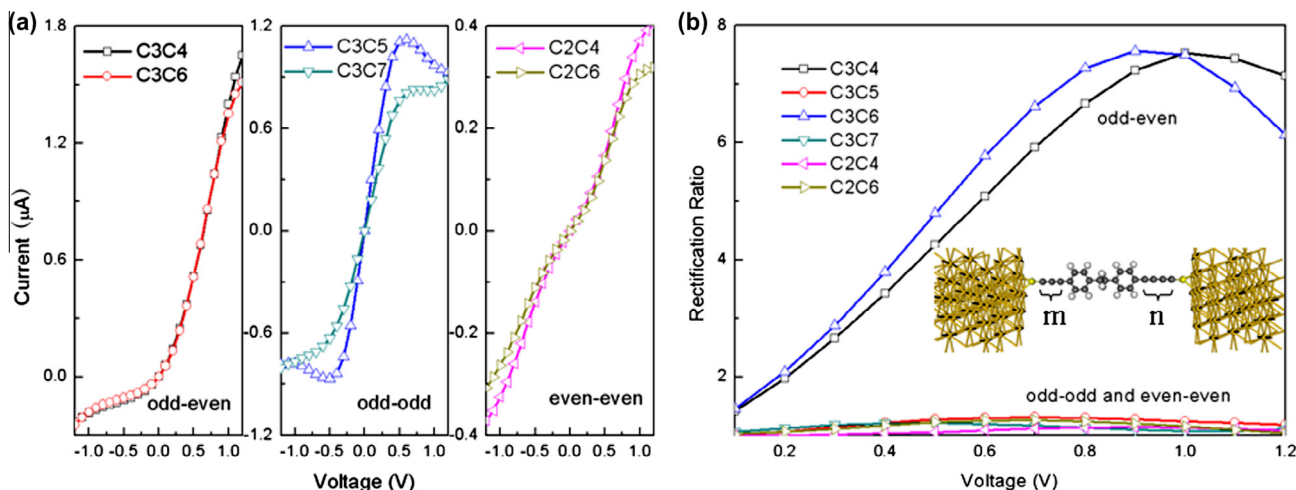

Figure 1. (a) The I–V curves of six models in our simulation in bias range from −1.2 to 1.2 V. (b) The corresponding rectification ratios change with bias. The inset shows the structures of six models: C3C4 ($m = 3$, $n = 4$), C3C5 ($m = 3$, $n = 5$), C3C6 ($m = 3$, $n = 6$), C3C7 ($m = 3$, $n = 7$), C2C4 ($m = 2$, $n = 4$) and C2C6 ($m = 2$, $n = 6$).